Hindawi
Journal of Control Science and Engineering
Volume 2022, Article ID 7696706, 8 pages
https://doi.org/10.1155/2022/7696706

Research Article

Coordinated Compliance Control Method of Five-Axis Redundant Industrial Manipulator Based on Monocular Vision

Hua Cen

Department of Mechanical and Electrical Engineering, Guangxi Modern Polytechnic College, Hechi 547000, China

Correspondence should be addressed to Hua Cen; cenhua@mju-edu.cn

Received 29 August 2022; Revised 26 October 2022; Accepted 29 October 2022; Published 23 November 2022

Academic Editor: Jiehao Li

In order to improve the accuracy of the five-axis redundant industrial robot arm in grasping static objects and shorten the grasping time, a coordinated compliance control method based on a monocular vision for the five-axis redundant industrial robot arm is proposed in this paper. Using the monocular vision ranging method, the three-dimensional coordinates of the target object in a base coordinate system of the five-axis redundant industrial robotic arm are calculated and object target positioning is achieved. According to the acquired object target position, the traditional Euler angle is used to calculate the actuator posture impedance at the end of the robotic arm, thereby realizing the coordinated compliant control of the five-axis redundant industrial manipulator. The simulation experiment results show that the proposed coordinated compliance control method for a five-axis redundant industrial manipulator based on monocular vision can successfully grasp the target object in the shortest time and has high practical value.

1. Introduction

At present, automation and intelligence are the mainstream of the development of modern industrial systems, and industrial robots have also become the main research directions in various countries. By applying robots to industrial production, it is possible to realize mechanical automation of industrial production and improve production efficiency [1]. Among various robots, the five-axis redundant industrial manipulator has been widely favored by virtue of its wide movement space and high flexibility. Robotics is a highly intersecting frontier subject, which has aroused the wide interest of people with different professional backgrounds (including mechanics, computer science and engineering, control theory and control engineering, electronic engineering, and artificial intelligence sociology). In robotics research, there is a major contradiction between the robot's high requirements for flexibility that can generate any force when operating in a specific contact environment as well as the robot's high requirements for position servo rigidity and mechanical structure rigidity when operating in free space. The contradiction of the robot's ability to comply with the contact environment is called compliance [2]. To solve this contradiction, robot experts at home and abroad have conducted a lot of compliance control research. How to improve the flexibility of the five-axis redundant industrial manipulator has become a new focus of attention. The flexibility of the robot arm refers to the ability of the robot arm to adapt to the external constraint environment. When the robot arm is in contact with the environment, the ability of the contact force generated to track the desired force is manifested as the flexibility of the robot arm. The compliance of the robotic arm can be divided into passive compliance and active compliance. Passive compliance refers to the use of a specific compliance device to make the robotic arm comply with changes in the environment. Although this method can simplify the design of the controller, it requires additional compliance devices and often cannot be used for the control of complex or high-precision tasks. Active compliance refers to the design of appropriate control strategies to achieve control of the contact force between the robotic arm and the environment. By combining with other advanced methods, the advantages of active compliance control can be maximized, so as to effectively deal with more

complex environments and make the manipulator's arm obtain better compliance ability, which has become the main direction of current research on manipulator compliance control [3].

In literature [4], a compliance control method for the end tool of a robotic arm based on impedance control is proposed. This method establishes the dynamic relationship between the pose of the end tool of the robotic arm and the contact force/torque by using the joint position/speed sensor and the wrist force sensor. Through measurement, the joint angle, joint angular velocity, and end contact force feedback are obtained, so that the end effector of the manipulator can produce corresponding compliant motion according to the feedback. The application of impedance control in complex and delicate end tools is studied, and position and posture are incorporated into compliance control. In the design of the device, the integrated control of the end position and attitude is realized. Finally, taking screw removal as an example, the proposed end compliance control law is simulated to verify the position and attitude control and contact force control. The simulation results show that the designed compliance controller can effectively control the contact force within a reasonable range, and realize the integrated control of position and attitude within a small error range. However, the static grabbing success rate of the target object in this method is low, resulting in a poor grabbing effect. In literature [5], a somatosensory robotic arm control method based on time series similarity is proposed for a six-degree-of-freedom serial robotic arm with 51 single-chip microcomputers as the main control board, Kinect Xbox One as the sensor by using the Kinect sensor to collect human movements without contact. The information is converted into control instructions, allowing the robotic arm to imitate and follow the movement of the human body. Through the bone data acquisition module, the coordinates of the bone joint points are collected, the joint angle is calculated and stored in the MySQL database, and the MySQL database is used as the main communication bridge. The sexual algorithm combines the bone data acquisition module and the robotic arm control module. The acquisition platform adds the joint angle data to the database, the control platform retrieves the joint angle data from the database, and the control module calculates the difference between the current time and the previous time and then matches it with the data in the database to identify the movement trajectory and automatically complete the remaining actions. The experimental results prove that this method can effectively reduce the time lag, smooth raw data, and automatically filter out abnormal data. However, the static capture time of the target object in this method is longer, resulting in lower capture efficiency.

Aiming at the problems of the above methods, this paper proposes a coordinated compliance control method for five-axis redundant industrial manipulators based on monocular vision. The premise of capturing the target is to determine the position of the object. Therefore, the monocular camera is used to locate the target from the background environment, so that the five-axis redundant industrial robotic arm can automatically determine the location of the target object, thereby completing the coordinated compliant control of the robotic arm and achieving high-precision crawl motion.

2. Coordinated Compliance Control Method of Five-Axis Redundant Industrial Manipulator Based on Monocular Vision

2.1. Object Localization Based on Monocular Vision. Visual ranging can be monocular or binocular. Binocular ranging equipment is expensive and complicated to install. Monocular ranging has the advantages of simple calibration, convenient installation, and high economic efficiency. The three-dimensional coordinates of the target object in the coordinate system of the five-axis redundant industrial manipulator base are obtained to achieve target positioning [6–8].

If the internal and external parameters of the camera are known, and the three-dimensional coordinates of the target point P are known, the unique coordinates of the target point on the imaging plane can be obtained. However, the image coordinates of a known target point cannot be uniquely calculated due to its three-dimensional coordinates in space, because a single camera can only obtain two-dimensional information about the target object, so the points on the two-dimensional imaging plane are different from the three-dimensional space, which meets the one-to-one correspondence [9, 10]. In view of such shortcomings, if some constraints can be used to make the points on the image correspond to the points in space one by one, then a single camera can be used to locate the target object in three dimensions. The experimental objects and environment of this study should follow the constraints below:

(1) The movement of the robot body platform is on the ground level

(2) The position of the camera can be measured and fixed

(3) The angle of the camera is known and fixed

Under the above conditions, according to the perspective projection and the solid geometric relationship, a monocular vision ground plane ranging model is obtained, as shown in Figure 1.

In Figure 1, the triangle ABU is the horizontal ground, the corresponding horizontal plane area within the ABCD camera's field of view, the intersection of the camera's optical axis OG and the horizontal plane is G, and the point I is the vertical projection of the point O on the ground. The horizontal plane coordinate system is defined with G as the origin and the front of the five-axis redundant industrial manipulator as the Y axis [11]. The points G, A, B, C, and D on the horizontal plane correspond to g, a, b, C, and d in the image, as shown in Figure 1(b), H and W are the camera's vertical resolution and horizontal resolution, respectively. Let the coordinate of any point P on the horizontal plane be (X_P, Y_P), and the corresponding point on the camera imaging plane is $p(x_p, y_p)$.

The imaging geometric relationship of the target point in the Y-axis direction is shown in Figure 2:

In Figure 2, it can be seen from the projection relationship that the triangle OEI is perpendicular to the horizontal plane. The intersection of the extension line of ML perpendicular to OG and the straight line fF is L. Py is the projection point of the point P on the y axis of the camera image coordinate system, P_y is the projection point of the point P on the y axis in the horizontal plane coordinate system, and z is the intersection point of the line PyP_y and the line ML [12, 13].

Assuming that the horizontal and vertical fields of view angles of the camera are known, which are $2\beta_0$ and $2\alpha_0$, respectively, the angle between the optical axis of the camera and the ground is γ_0, and the vertical distance OI between the lens center O and the ground is h, so we have

$$\begin{aligned} \alpha &= \arctan\left(\frac{2y_p \tan(\alpha_0)}{H}\right), \\ OG &= \frac{h}{\cos\gamma_0}, \\ IG &= h * \tan\gamma_0, \\ IP_y &= h * \tan(\gamma_0 + \alpha). \end{aligned} \tag{1}$$

In the horizontal plane coordinate system, the value of GP_y is the coordinate Y_P of P in the direction of the Y axis so that

$$Y_P = h(\tan(\gamma_0 + \alpha) - \tan\gamma_0). \tag{2}$$

In triangle IGO, $IG = h * \tan\gamma_0$, $IF = h * \tan(\gamma_0 - \alpha_0)$, so we have

$$GF = h(\tan\gamma_0 - \tan(\gamma_0 - \alpha_0)). \tag{3}$$

Simultaneously $OG = h/\cos\gamma_0$, $OF = h/\cos(\gamma_0 - \alpha_0)$, we have

$$\begin{aligned} GJ &= \frac{h}{\cos\gamma_0} * \tan\beta_0, \\ FC &= \frac{h}{\cos(\gamma_0 - \alpha_0)} * \tan\beta_0. \end{aligned} \tag{4}$$

From the similarity of triangle UFC and UGJ, we can get

$$\begin{aligned} UG = \frac{UF * GL}{FC} &= \frac{(h/\cos\gamma_0) * \tan\beta_0 * h(\tan\gamma_0 - \tan(\gamma_0 - \alpha_0))}{(h/\cos\gamma_0) * \tan\beta_0 - (h/\cos(\gamma_0 - \alpha_0)) * \tan\beta_0} \\ &= \frac{\cos(\gamma_0 - \alpha_0) * h(\tan\gamma_0 - \tan(\gamma_0 - \alpha_0))}{\cos(\gamma_0 - \alpha_0) - \cos\gamma_0}. \end{aligned} \tag{5}$$

In the horizontal plane triangle ABU, we can obtain the following formula according to the triangle similarity theorem:

$$\begin{aligned} X_P &= \frac{GL * (UG + Y_P)}{UG} \\ &= \frac{UG + Y_P}{UG} * \frac{h}{\cos\gamma_0} * \frac{2 * x_p * \tan\beta_0}{W}. \end{aligned} \tag{6}$$

From the triangle relationship, the distance from the camera to the target object is

$$OP = \sqrt{OI^2 + IP^2} = \sqrt{h^2 + X_P^2 + (Y_P + h * \tan\gamma_0)^2}. \tag{7}$$

After obtaining the three-dimensional coordinates of the target object in the ground coordinate system through the monocular ranging algorithm, the target object in the five-axis redundancy can be obtained through coordinate system transformation from the ground coordinate system to the five-axis redundant industrial robot base coordinate system. The transformation formula of the three-dimensional coordinates in the coordinate system of the industrial robot arm base is as follows:

$${}^0PD = \frac{{}^0_W T\, {}^W PD}{OP}, \tag{8}$$

where ${}^W PD$, ${}^0 PD$ are the three-dimensional coordinates of the target object in the ground coordinate system and the five-axis redundant industrial robotic arm base coordinate system, respectively. ${}^0_W T$ is the transformation matrix from the ground coordinate system to the five-axis redundant industrial robotic arm base coordinate system [14, 15].

According to the acquired three-dimensional coordinates of the target object in the robot arm base coordinate system, the target positioning of the object is realized, which provides environmental information for the subsequent coordinated compliance control of the five-axis redundant industrial robot arm.

2.2. Impedance Control of Robotic Arm-Compliant Motion. After obtaining the target position of the object through monocular vision ranging, impedance control is performed

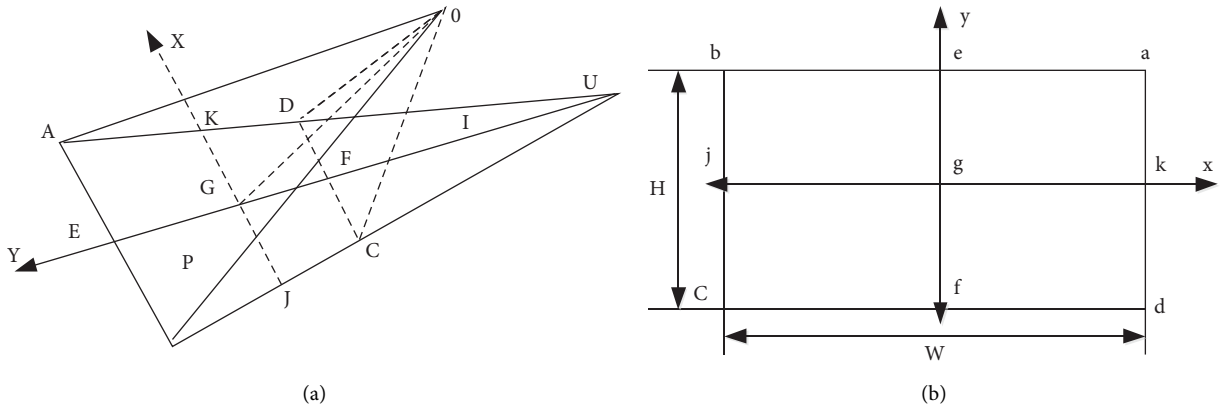

Figure 1: Ground projection model and camera image plan.

on the compliant motion of the five-axis redundant industrial manipulator. The impedance control does not directly control the force of the robot in the environment. In fact, according to the relationship between the position, speed, and acceleration of the robot end and the interaction force between the end of the robot and the environment, the goal of controlling the force is achieved by adjusting the target impedance even though the end of the robot achieves a smooth motion. So, in a sense, impedance control can be regarded as an extension of position control.

When the manipulator is in a stable state, selecting a low-weight parameter matrix $K_p^{-1}K_M$ can achieve effective anti-interference, which is equivalent to the stiffness control of the lightweight end effector. When the end effector is in contact with a more rigid environment, the end effector's flexibility will be eventually affected, and the solution to separate motion control from impedance control. The purpose of motion control is to improve stiffness, thereby enhancing the anti-interference ability. Rather than ensuring accurate tracking of the desired end effector trajectory, it should be ensuring accurate tracking of the reference position and direction generated by the impedance control action. In other words, the desired trajectory and the acquired contact force and torque are used as the input for impedance control, and then a new position and posture are generated through appropriate integration as the motion control reference input.

In addition to the desired coordinate system, it is necessary to introduce a reference coordinate system using p_d and R_d, respectively. This coordinate system is called a flexible coordinate system, which is specified by the position vector p_c and the rotation matrix R_c. In this way, only the actual end effector position p_e and posture R_e and R_c and R_c are consistent, and the inverse dynamic motion control strategy is still available. Similarly, the actual linear velocity p_e' and angular velocity ω_e of the end effector correspond to p_c' and ω_c, respectively.

To realize a solid physical interaction between the end effector and the environment, the following equation needs to be satisfied:

$$M_P\Delta p_{dc}' + D_P\Delta p_{dc}' + K_P\Delta p_{dc}' = f, \tag{9}$$

where p_d represents the desired trajectory, which is a constant. M_P and K_P are symmetric matrices. By calculating the inertial force generated by the rigid body with mass m_P, then the kinetic energy of the entire robotic arm is as follows:

$$T_p = \frac{1}{2}{}^0 PDm_p p_c'. \tag{10}$$

Secondly, the variable to be calculated is the dissipative damping force. The last variable represents the force acting on the linkage of the robotic arm. The force is composed of the stiffness matrix K_P and the desired trajectory p_d. The potential energy of the entire robotic arm is as follows:

$$U_p = \frac{1}{2}T_p\Delta p_{dc}' K_P. \tag{11}$$

In order to ensure the successful execution of interactive tasks, the end effector has a suitable compliant behavior. The choice of the stiffness matrix is crucial. Therefore, it is necessary to analyze the elastic items from the collective perspective. The stiffness matrix K_P can be decomposed into

$$K_P = U_p\Gamma_p U_p, \tag{12}$$

where Γ_p, U_p are the eigenvalue matrix and eigenvector matrix, respectively.

By further considering the impedance of the rotating part, that is, the posture impedance of the end effector of the robotic arm, the rotational impedance equation is calculated by using the traditional Euler angle.

$$T = \Delta\varphi_{dc}\left(M_0 + D_0 + K_0\right), \tag{13}$$

where M_0, D_0, K_0, respectively represent the generalized inertia tensor, rotational impedance, and rotational stiffness, which constitute a positive definite matrix. $\Delta\varphi_{dc}$ represents the moment in the compliant coordinate system.

3. Simulation Experiment Analysis

3.1. Experimental Platform Equipment and Parameter Settings. In order to verify the performance of the proposed coordinated compliance control method for the five-axis

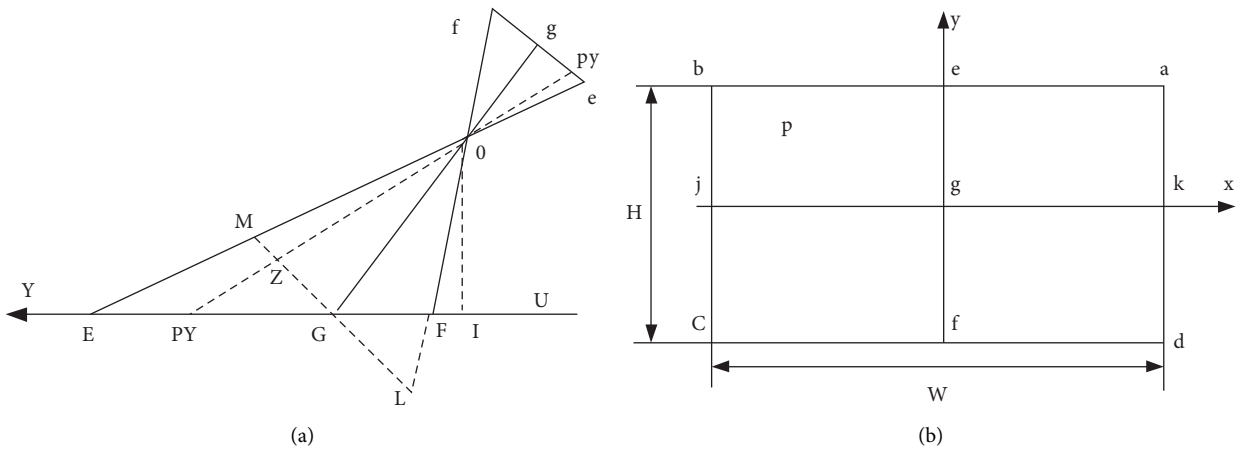

Figure 2: The imaging geometry of the target point in the Y-axis direction.

Figure 3: The experimental platform device for the five-axis redundant industrial robotic arm.

redundant industrial manipulator based on the monocular vision in practical applications, simulation experiments are performed based on Simulink in MATLAB software. The experimental platform device for the five-axis redundant industrial manipulator is shown in Figure 3.

In this paper, SC-A850HLS5 five-axis redundant manipulator is selected as the research object, and its specific parameters are shown in Table 1.

The basic parameter settings of the robotic arm are shown in Table 1.

Table 1: Basic parameters of the robotic arm.

Category	Explain
Joint type	Rotating joint
Body mass	330 kg
Payload	15 kg
Drive mode	Servomotor
Basic materials	Aluminum alloy

3.2. Test Subject. The practical performance of the proposed method is evaluated by taking the grab success rate and grab time as the evaluation indicators. Select 6 target objects as experimental objects, and place them on the same level as the five-axis redundant industrial manipulator experimental platform. The experimental objects are shown in Figure 4:

3.3. Crawl Success Rate. The proposed five-axis redundant industrial manipulator coordinated compliance control method based on monocular vision, the compliance control method of the end tool based on impedance control proposed in the literature [4], and the time series similarity based on the literature [5] are comparatively analyzed. Three methods are used to carry out static grasping experiments on six kinds of target objects, namely, the manipulator grabs the designated target in the platform, and each experiment is carried out 30 times. If the target object is not captured successfully within 30 s, that is, the surrounding objects are captured or touched, the capture is judged as failed. For each group of experiments, calculate the number of successful captures, the number of failed captures, and the success rates. The experimental statistical results are shown in Tables 2–4.

According to the data in Tables 2–4, the proposed method has 30 successful grasps and 0 fails, with a success rate of 100%. For the method proposed in the literature [4], the number of successful grasps of the six target objects is about 26–28, and the highest success rate is only 93.3%. For the method in literature [5], the number of successful grasps of six target objects is about 25~26, and the highest success rate is 86.6%. The results show that this

Figure 4: Experimental object.

Table 2: Experimental results of static crawling when using the proposed method.

Goods	Success times (times)	Failure times (time)	Success rate (%)
A	30	0	100
B	30	0	100
C	30	0	100
D	30	0	100
E	30	0	100
F	30	0	100

Table 3: Results of static capture experiment of the method in literature [4].

Goods	Success times (times)	Failure times (time)	Success rate (%)
A	27	3	90.0
B	26	4	86.6
C	28	2	93.3
D	28	2	93.3
E	28	2	93.3
F	26	4	86.6

Table 4: The experimental results of the static grabbing using the method in literature [5].

Goods	Success times (times)	Failure times (time)	Success rate (%)
A	25	5	83.3
B	26	4	86.6
C	25	5	83.3
D	26	4	86.6
E	25	5	83.3
F	25	5	83.3

method is superior to the other two methods, and will not touch the surrounding objects during the static capture of the target. This is mainly because this method uses the monocular vision ranging method to calculate the position of the target object in the five-axis redundancy. According to the three-dimensional coordinates in the basic coordinate system of the industrial robot arm, the object and target can be accurately located.

3.4. Crawl Time. The proposed method as the methods in the literature [4, 5] is comparatively analyzed in terms of crawling time, and the comparison results are shown in Figure 5.

According to Figure 5, the proposed method realizes static grasping of the target object within 11 s, while the grasping time of the method in literature [4, 5] is 13 s and 14 s, which shows that the static grasping time of the target object of the proposed method is shorter.

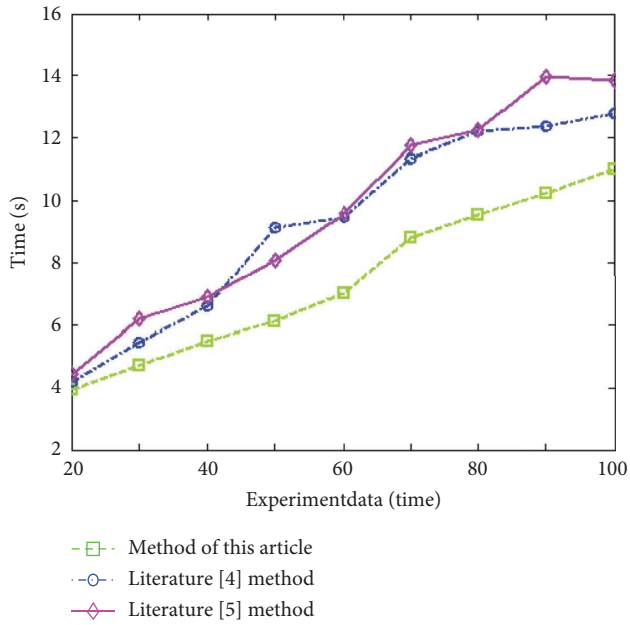

Figure 5: Comparison results of crawling time of three methods.

4. Conclusions

For a new generation of interactive robots, the control of the manipulator is extremely important. Aiming at the problems of long static grasping time and low grasping success rate of the traditional coordinated compliance control method, a coordinated compliance control method of a five-axis redundant industrial manipulator based on monocular vision is proposed. This method uses a monocular vision ranging method to calculate the three-dimensional coordinates of the target object, so as to achieve rapid and accurate target positioning. Then, according to the target position obtained, the traditional Euler angle computer is used to calculate the attitude impedance of the end effector of the robot arm, so as to realize the coordinated control of the five-axis manipulator. Finally, the simulation experiment is conducted to prove the practicability of the proposed method. According to the comparison results, the method proposed in this paper can successfully capture the static target with a success rate of 100%, and its static capture time is less than 11 s, showing high capture efficiency and great application value.

Data Availability

The datasets used and/or analyzed during the current study are available from the corresponding author upon reasonable request.

Conflicts of Interest

The authors declare that there are no conflicts of interest regarding this article.

Acknowledgments

This research has been financed by 2021 Guangxi Universities Young and Middle-Aged Teachers Research Foundation Ability Improvement Project "based on FANUC system three axis CNC milling machine upgrade research" (No. 2021KY1420) and "Design and research of virtual simulation system of robot disassembly and assembly practical training based on Unity3D software platform" of the project of 2022 for the improvement of scientific research basic ability of young and middle-aged teachers in Guangxi Universities (No. 2022KY1438).

References

[1] E. Kopperger, J. List, S. Madhira, F. Rothfischer, D. C. Lamb, and F. C. Simmel, "A self-assembled nanoscale robotic arm controlled by electric fields," *Encephale*, vol. 359, no. 6373, pp. 296–310, 2018.

[2] C. Nan, "Research on the robotic arm control system based on the reconfiguration technology," *International English Education Research: English Edition*, vol. 6, no. 3, pp. 6–8, 2019.

[3] D. Banerjee and K. Yu, "Integrated test automation for evaluating a motion-based image capture system using a robotic arm," *IEEE Access*, vol. 7, pp. 1888–1896, 2019.

[4] H. Li, F. W. Wang, S. J. Xu, Y. Y. Hou, and S. Lu, "Compliance control of end tool of manipulator based on impedance control," *Space Control Technology and Application*, vol. 45, no. 01, pp. 23–29, 2019.

[5] S. Q. Hu, H. Y. Yuan, J. C. Zou, Y. L. Shi, X. M. Liu, and X. Q. Meng, "Research on control system of somatosensory robot arm based on time series similarity," *Power System and Control*, vol. 7, no. 4, pp. 287–297, 2018.

[6] R. Satheeshkumar, "Real time robotic arm control using human hand gesture measurement," *Journal of Advanced Research in Dynamical and Control Systems*, vol. 12, no. SP4, pp. 984–996, 2020.

[7] L. Barbieri, F. Bruno, A. Gallo, M. Muzzupappa, and M. L. Russo, "Design, prototyping and testing of a modular small-sized underwater robotic arm controlled through a master-slave approach," *Ocean Engineering*, vol. 158, no. 15, pp. 253–262, 2018.

[8] S. Bularka, R. Szabo, M. Otesteanu, and M. Babaita, "Robotic arm control with hand movement gestures," in *Proceedings of the 2018 41st International Conference on Telecommunications and Signal Processing (TSP)*, pp. 1–5, Athens, Greece, July 2018.

[9] J. H. Jeong, K. H. Shim, D. J. Kim, and S. W. Lee, "Brain-controlled robotic arm system based on multi-directional CNN-BiLSTM network using EEG signals," *IEEE Transactions on Neural Systems and Rehabilitation Engineering*, vol. 28, no. 5, pp. 1226–1238, 2020.

[10] Q. Xu, L. Xing, Y. Zhao, T. Jia, and Y. Huang, "A source stirred reverberation chamber using a robotic arm," *IEEE Transactions on Electromagnetic Compatibility*, vol. 62, no. 2, pp. 631–634, 2020.

[11] J. Gao, Y. Chen, and F. Li, "Kinect-based motion recognition tracking robotic arm platform," *Intelligent Control and Automation*, vol. 10, no. 03, pp. 79–89, 2019.

[12] M. DiPierro, "Toy vision-guided 3D robotic arm in Javascript," *Computing in Science & Engineering*, vol. 20, no. 1, pp. 43–49, 2018.

[13] A. A. Alhamadani and M. Z. Al-Faiz, "Inverse kinematic based brain computer interface to control humanoid robotic arm," *International Journal of Mechanical & Mechatronics Engineering*, vol. 20, no. 1, pp. 15–24, 2020.

[14] M. Abdelaal, A. Bahgat, H. M. Emara, and A. El-Dessouki, "Real-time external control coupled with vision-based control for an industrial robotic arm to pick and place moving object on a conveyor belt," *International Journal of Mechanical & Mechatronics Engineering*, vol. 19, no. 1, pp. 123–131, 2019.

[15] Y. Z. Hsieh and S. S. Lin, "Robotic arm assistance system based on simple stereo matching and q-learning optimization," *IEEE Sensors Journal*, vol. 20, no. 18, pp. 10945–10954, 2020.